$\mathbb{Z}_3$ Parafermion in the Double Charge Kondo Model

D. B. Karki,[1,*] Edouard Boulat,[2] Winston Pouse,[3,4] David Goldhaber-Gordon,[4,5]
Andrew K. Mitchell,[6,7,†] and Christophe Mora[8,‡]

[1]*Division of Quantum State of Matter, Beijing Academy of Quantum Information Sciences, Beijing 100193, China*
[2]*Université de Paris, CNRS, Laboratoire Matériaux et Phénomènes Quantiques, 75013 Paris, France*
[3]*Department of Applied Physics, Stanford University, Stanford, California 94305, USA*
[4]*SLAC National Accelerator Laboratory, Menlo Park, California 94025, USA*
[5]*Department of Physics, Stanford University, Stanford, California 94305, USA*
[6]*School of Physics, University College Dublin, Belfield, Dublin 4, Ireland*
[7]*Centre for Quantum Engineering, Science, and Technology, University College Dublin, Ireland*
[8]*Université Paris Cité, CNRS, Laboratoire Matériaux et Phénomènes Quantiques, 75013 Paris, France*

(Received 10 October 2022; accepted 1 February 2023; published 6 April 2023)

Quantum impurity models with frustrated Kondo interactions can support quantum critical points with fractionalized excitations. Recent experiments [W. Pouse *et al.*, Nat. Phys. (2023)] on a circuit containing two coupled metal-semiconductor islands exhibit transport signatures of such a critical point. Here, we show using bosonization that the double charge-Kondo model describing the device can be mapped in the Toulouse limit to a sine-Gordon model. Its Bethe-ansatz solution shows that a $\mathbb{Z}_3$ parafermion emerges at the critical point, characterized by a fractional $\frac{1}{2}\ln(3)$ residual entropy, and scattering fractional charges $e/3$. We also present full numerical renormalization group calculations for the model and show that the predicted behavior of conductance is consistent with experimental results.

DOI: 10.1103/PhysRevLett.130.146201

Quantum impurity models, which feature a few localized, interacting quantum degrees of freedom coupled to noninteracting conduction electrons, constitute an important paradigm in the theory of strongly correlated electron systems [1]. They describe magnetic impurities embedded in metals or other materials [2,3], and nanoelectronic devices such as semiconductor quantum dots [4–6] or single-molecule transistors [7,8]. They are also central to the understanding of bulk correlated materials through dynamical mean field theory [9]. Generalized quantum impurity models host a rich range of complex physics, including various Kondo effects [10–19] and quantum phase transitions [20–29]. Such models provide a simple platform to study nontrivial physics which can be difficult to identify in far more complex bulk materials. Indeed, exact analytical and numerical methods for quantum impurity models have given deep insights into strong correlations at the nanoscale [30–34].

The two-channel Kondo (2CK) [10,23] and two-impurity Kondo (2IK) [21,22] models are classic examples in which frustrated interactions give rise to non-Fermi liquid physics at quantum critical points (QCPs) with fractionalized excitations. The seminal work of Emery and Kivelson (EK) [32] solved the 2CK model in the Toulouse limit using bosonization techniques, and understood the QCP in terms of a free Majorana fermion localized on the impurity. In the 2IK model [22,35–39], a free Majorana arises from the competition between a Ruderman-Kittel-Kasuya-Yosida (RKKY) exchange interaction coupling the impurities, and individual impurity-lead Kondo effects. In both cases the QCP is characterized by a finite, fractional residual impurity entropy of $\frac{1}{2}\ln(2)$ [22,31], which is a distinctive fingerprint of the free Majorana.

Semiconductor quantum devices [4–6] can constitute experimental quantum simulators for such impurity models, with *in situ* control over parameters allowing correlated electron phenomena to be probed with precision. The distinctive conductance signatures predicted [24,36,37] for the 2CK model at criticality were since observed [25,27] (although the 2IK model has never been realized [40]). More recently, Matveev's charge Kondo paradigm [41,42] has emerged as a viable alternative to engineer exotic states, with both 2CK [28] and its three-channel variant [29] being realized experimentally.

Given the intense experimental efforts to demonstrate the existence of Majoranas in quantum devices [43,44], and the broader interest in realizing anyons for the purposes of quantum computing [45,46], the Kondo route to fractionalization has gained traction [47–50]. Experimental circuit realizations of more complex quantum impurity models offer the tantalizing opportunity to produce more exotic anyons in tunable nanoelectronics devices. This can be viewed as part of a wider effort to study fractionalization in condensed matter systems [51–57].

However, despite the suggestive fractional entropies in certain Kondo-type models [29–31,58–61], the *explicit* construction of parafermion operators in these systems has not previously been possible. This is because—unlike for the simpler case of Majoranas—parafermions cannot arise in an effective free fermion system. Applying the EK method yields an irreducibly strongly interacting model, which has hitherto hindered finding exact solutions in which free local parafermions could be identified.

In this Letter, we study the double charge-Kondo (DCK) model describing a very recent experiment [60] involving two hybrid metal-semiconductor islands coupled together in series, and each coupled to its own lead, at quantum point contacts (QPCs)—see Fig. 1. The DCK model is a variant of the celebrated 2IK model, but with an interisland Kondo interaction rather than an RKKY exchange interaction [21]. At the triple point in the charge stability diagram of the device, a QCP was found to arise due to the competition between island-lead Kondo and interisland Kondo [60]. Numerical renormalization group [33,34,72,73] (NRG) calculations for the DCK model showed a fractional residual entropy of $\frac{1}{2}\ln(3)$ at the QCP—suggesting an unusual anyonic state (and not simply a Majorana). The same critical point and fractional entropy were identified analytically near perfect QPC transmission [74], although no Kondo effects occur in this limit.

Here, we examine the "Kondo" case of weak-to-intermediate transmission, and apply the EK mapping [32] in the Toulouse limit. Even though the EK method yields a highly nontrivial interacting model, we show that it can nevertheless be solved using Bethe ansatz. Instead of the free Majorana found by EK for the 2CK model, we explicitly establish the existence of a $\mathbb{Z}_3$ parafermion in the DCK model, and identify it as the source of the $\frac{1}{2}\ln(3)$ residual entropy. Analytic expressions for conductance near the QCP are also extracted, and we show that experimental transport data are consistent with these predictions. To complete the theoretical description, we obtain the full temperature dependence of entropy and conductance via NRG, which does not rely on the Toulouse approximation.

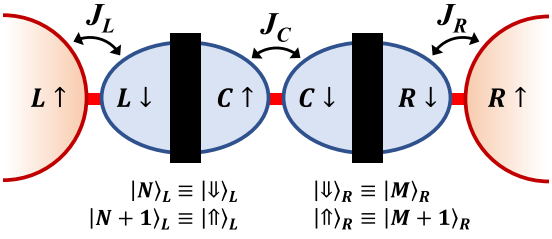

FIG. 1. Schematic of the two-site charge Kondo circuit described by the DCK model. Two hybrid metal-semiconductor islands are coupled to each other and to their own lead at QPCs. Macroscopic island charge states mapped to pseudospin degrees of freedom are flipped by tunneling at QPCs.

System and model.—The two-island circuit illustrated in Fig. 1 is described by the DCK model at low temperatures $T \ll E_C$ (with E_C the island charging energies) for weak-to-intermediate QPC transmissions, see Ref. [60]:

$$H_{\rm DCK} = (J_L S_L^+ s_L^- + J_R S_R^+ s_R^- + J_C S_R^+ S_L^- s_C^- + \text{H.c.}) - h_L S_L^z - h_R S_R^z + I S_L^z S_R^z + H_{\rm elec}, \quad (1)$$

where $H_{\rm elec} = \sum_{\alpha,\sigma,k} \epsilon_k \psi^\dagger_{\alpha\sigma k}\psi_{\alpha\sigma k}$ describes the electronic reservoirs either side of QPC $\alpha = L, C, R$. Although the physical electrons are spin polarized [60], we label electrons on the lead or island either side of QPC L, R as $\sigma = \uparrow$ or $\downarrow$, and island electrons to the left or right of the central QPC C as $\sigma = \uparrow$ or $\downarrow$—see Fig. 1. We assume linear dispersion $\epsilon_k = v_F k$, with momentum k. We then define pseudospin operators $s_\alpha^- = \psi^\dagger_{\alpha\downarrow}(0)\psi_{\alpha\uparrow}(0)$ and $s_\alpha^+ = (s_\alpha^-)^\dagger$, where $\psi_{\alpha\sigma}(0)$ is defined at the QPC position. Confining our attention to the lowest two macroscopic charge states of each island $|n,m\rangle \equiv |n\rangle_L \otimes |m\rangle_R$, with $n = N, N+1$ the number of electrons on the left island and $m = M, M+1$ electrons on the right island, we introduce "impurity" charge pseudospin operators $S_L^+ = \sum_m |N+1,m\rangle\langle N,m|$, $S_L^z = \sum_m \frac{1}{2}[|N+1,m\rangle\langle N+1,m| - |N,m\rangle\langle N,m|]$, $S_R^+ = \sum_n |n,M+1\rangle\langle n,M|$, $S_R^z = \sum_n \frac{1}{2}[|n,M+1\rangle\langle n,M+1| - |n,M\rangle\langle n,M|]$, and $S_\alpha^- = (S_\alpha^+)^\dagger$. The first line in Eq. (1) therefore corresponds to tunneling processes at the three QPCs (with the tunneling amplitude J_α being related to the transmission τ_α of QPC α). Gate voltages on the islands control $h_{L,R}$ and allow the charge stability diagram to be navigated. I is a capacitive interaction between the two islands. For $J_{L,C,R} = I = 0$, the four retained charge configurations $|n,m\rangle$ are degenerate when $h_L = h_R = 0$. However, a finite J_C and/or I partially lifts this degeneracy to yield a pair of separated triple points (TPs) in gate voltage space. As with the experiment [60], here we focus on the vicinity of the TP at which the charge configurations $|N,M\rangle/|N+1,M\rangle/|N,M+1\rangle$ are degenerate. We hereafter neglect the term I, since it just renormalizes the TP splitting already induced by $J_C > 0$ and is otherwise irrelevant [74]. The rest of this Letter is devoted to the nontrivial Kondo competition arising when the couplings to the leads are switched on, $J_{L,R} > 0$.

QCP.—At the TP, the three "impurity" states (the degenerate charge configurations of the two-island structure) are interconverted by tunneling at the three QPCs:

$$|N,M\rangle \overset{J_L}{\leftrightarrow} |N+1,M\rangle \overset{J_C}{\leftrightarrow} |N,M+1\rangle \overset{J_R}{\leftrightarrow} |N,M\rangle.$$

The accompanying conduction electron pseudospin-flip scattering at each QPC described by the operators $s^\pm_{L,C,R}$ in Eq. (1) give rise to competing Kondo effects. Since island-lead and interisland Kondo effects cannot be

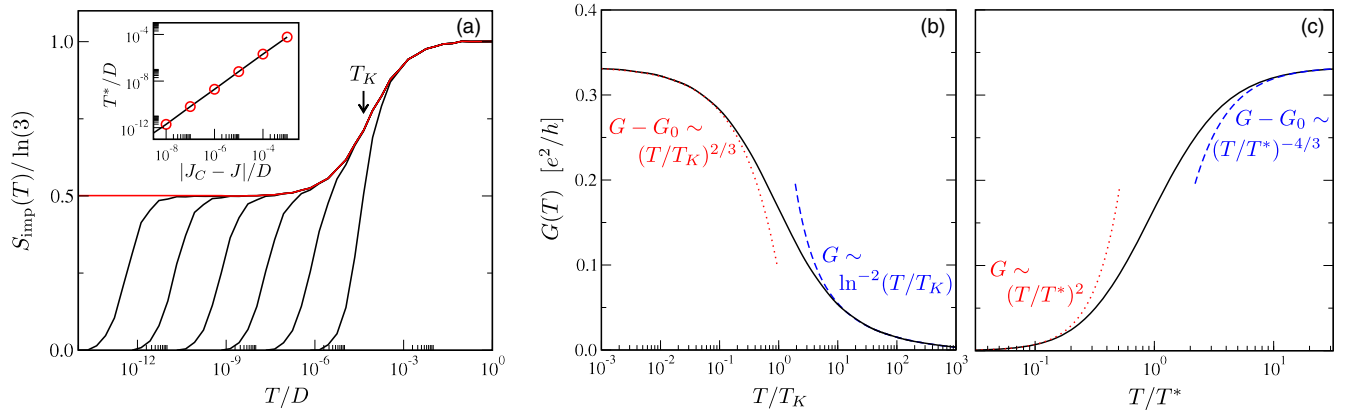

FIG. 2. NRG results at the triple point of the DCK model. (a) Entropy $S_{\rm imp}(T)$ in the vicinity of the critical point, showing the flow $\ln(3) \to \frac{1}{2}\ln(3)$ on the Kondo scale T_K, and subsequently $\frac{1}{2}\ln(3) \to 0$ on the Fermi liquid scale T^*. Plotted for $J/D = 0.2$ and $|J_C - J|/D = 10^{-3}, 10^{-4}, \ldots, 10^{-8}$ (black lines) approaching the critical point $J_C = J$ (red line). D is the conduction electron bandwidth. The inset shows the power-law behavior Eq. (2). (b) Universal conductance curve as a function of T/T_K at the critical point. (c) Universal Fermi liquid crossover as a function of T/T^*. Conductance asymptotes are discussed in the text.

simultaneously satisfied, a frustration-driven QCP arises when $J_L = J_R = J_C$, as reported in Refs. [60,74].

NRG solution.—In Fig. 2 we present numerically exact results for the DCK model tuned to the TP, obtained by NRG [33,34,72,73] (see [61] for details). We set $J_L = J_R \equiv J$ and vary J_C in the vicinity of the QCP arising when $J_C = J$. In panel (a) we show the impurity contribution to the entropy $S_{\rm imp}$ as a function of temperature T. The critical point $J_C = J$, shown as the red line, exhibits Kondo "overscreening" to a non-Fermi liquid state on the scale of T_K. The three degenerate charge states give a high-T entropy of ln(3), but the entropy is partially quenched to $\frac{1}{2}\ln(3)$ for $T \ll T_K$. Introducing channel anisotropy $J_C \neq J$ induces a Fermi liquid (FL) crossover on the lower scale of T^*, below which the entropy is completely quenched. The inset shows the extracted power-law behavior,

$$T^*/T_K \sim (|J_C - J|/T_K)^{3/2}. \tag{2}$$

The same form was reported for detuning away from the TP in Ref. [60]. For $|J_C - J| \ll T_K$ we have good scale separation $T^* \ll T_K$, such that the crossover to the critical point is a universal function of the single scaling parameter T/T_K, whereas the crossover away from it is a universal function of only T/T^*. This is reflected in the behavior of series conductance, shown in panels (b),(c). At the highest temperatures $T \gg T_K$, Kondo-renormalized spin-flip scattering gives standard $\ln^{-2}(T/T_K)$ corrections to conductance; whereas on the lowest temperature scales $T \ll T^*$, we observe conventional FL scaling of conductance $\propto (T/T^*)^2$. Much more interesting is the behavior in the vicinity of the critical fixed point [60],

$$G_0 - G(T) \sim (T/T_K)^{2/3}, \quad T \ll T_K\,, \tag{3a}$$

$$G_0 - G(T) \sim (T/T^*)^{-4/3}, \quad T \gg T^*\,, \tag{3b}$$

with $G_0 = e^2/3h$. Equations (2) and (3) are also obtained analytically and discussed in the following.

Bosonization and Toulouse point.—We now turn to the details of our exact solution. Following EK [32], we bosonize the conduction electron Hamiltonian $H_{\rm elec}$ and obtain a simplified model in the Toulouse limit after applying a unitary transformation.

As a first step, we write $\psi_{\alpha\sigma} = e^{i\phi_{\alpha\sigma}}/\sqrt{a}$ with $a = 4\pi v_F \equiv 1$ and introduce three chiral bosonic fields $\delta\phi_\alpha \equiv (\phi_{\alpha\uparrow} - \phi_{\alpha\downarrow})/\sqrt{2}$ for $\alpha = L, R, C$. The conduction electron pseudospin operators follow as $s^-_\alpha = e^{i\sqrt{2}\delta\phi_\alpha}$, and

$$H_{\rm elec} = \frac{v_F}{4\pi}\sum_\alpha \int dx \left(\frac{\partial\delta\phi_\alpha}{\partial x}\right)^2. \tag{4}$$

For $h_L = h_R = I = 0$, we can cast the DCK model as

$$H_{\rm DCK} = H_{\rm elec} + \Big[J_L S^+_L e^{i\sqrt{2}\delta\phi_L} + J_R S^+_R e^{i\sqrt{2}\delta\phi_R} + J_C S^+_R S^-_L e^{i\sqrt{2}\delta\phi_C} + \text{H.c.}\Big], \tag{5}$$

where all fields are implicitly taken at $x = 0$. To make progress, we deform the original DCK model, which features only transverse couplings J_α, by adding an Ising term $\bar{H}_{\rm DCK} = H_{\rm DCK} + H_I$. Since pseudospin anisotropy is RG irrelevant, H_I affects only the flow, not the stable fixed point itself. Therefore, the critical fixed point (and indeed the entire FL crossover in the limit $T^* \ll T_K$ [36,37]) is the same for any choice of H_I. We shall exploit this property to identify an exactly solvable Toulouse limit. To do this we effect a change of basis,

$$\delta\phi_A = (\delta\phi_R - \delta\phi_C - \delta\phi_L)/\sqrt{3},$$
$$\delta\phi_B = (\delta\phi_L + \delta\phi_R)/\sqrt{2},$$
$$\delta\phi_D = (\delta\phi_L - 2\delta\phi_C - \delta\phi_R)/\sqrt{6}, \quad (6)$$

and introduce $\delta\phi_{1/2} = (\delta\phi_B/\sqrt{2}) \pm (\delta\phi_D/\sqrt{6})$. We now choose

$$H_I = \lambda[S_L^z \partial_x \delta\phi_1(0) + S_R^z \partial_x \delta\phi_2(0)] \quad (7)$$

and rotate the Hamiltonian into $U\bar{H}_{\mathrm{DCK}}U^\dagger = H_{\mathrm{elec}} + H_{\mathrm{EK}}$ using the EK unitary transformation [32]

$$U = \exp\left[-i\frac{1}{\sqrt{2}}\{S_L^z \delta\phi_1(0) + S_R^z \delta\phi_2(0)\}\right]. \quad (8)$$

We then obtain

$$H_{\mathrm{EK}} = \left[J_L S_L^- + J_R S_R^+ + J_C S_L^+ S_R^-\right] e^{i\sqrt{2/3}\delta\phi_A} + \mathrm{H.c.}$$
$$+ \bar{\lambda}\left[S_L^z \partial_x \delta\phi_1(0) + S_R^z \partial_x \delta\phi_2(0)\right], \quad (9)$$

where $\bar{\lambda} = \lambda - 1/(4\pi)^2$. The Toulouse limit is obtained by setting $\bar{\lambda} = 0$, for which the bosonic modes $\delta\phi_{B,D}$ fully decouple and remain free. The symmetric charge mode $\delta\phi_A$ thus controls the low-energy behavior following Kondo screening. At the QCP with isotropic couplings $J_L = J_R = J_C \equiv J$, the model further simplifies,

$$H_{\mathrm{EK}} = J\sigma e^{i\sqrt{2/3}\delta\phi_A} + \mathrm{H.c.}, \quad \sigma = \begin{pmatrix} 0 & 1 & 0 \\ 0 & 0 & 1 \\ 1 & 0 & 0 \end{pmatrix}, \quad (10)$$

where the operator σ circularly permutes the three impurity states $|N, M\rangle/|N+1, M\rangle/|N, M+1\rangle$.

Parafermion modes.—In analogy with the description of chiral Potts (clock) models by parafermionic chains [75], we define a second operator $\tau = \mathrm{diag}(1, \omega, \omega^2)$, with $\omega = e^{2i\pi/3}$ in the impurity subspace. The operators [75,76] σ and $\sigma' = \sigma\tau$ then obey the parafermionic properties,

$$\sigma^3 = \sigma'^3 = 1, \qquad \sigma\sigma' = \omega\sigma'\sigma, \quad (11)$$

and thereby generalize the Majorana operators to a three-dimensional space with circular $\mathbb{Z}_3$ symmetry.

Importantly, H_{EK} in Eq. (10) includes only the terms σ and $\sigma^\dagger$, and not σ'. Since $\sigma\sigma^\dagger = \sigma^\dagger\sigma$, the parafermion σ commutes with H_{EK} and remains *free*. Conversely, σ' does not commute and it acquires a finite scaling dimension.

Sine-Gordon model and Bethe-ansatz solution.—We rotate to the simultaneous eigenbasis of σ and $\sigma^\dagger$ and write $H_{\mathrm{EK}} = H^0 \oplus H^+ \oplus H^-$, with

$$H^r = 2J\cos\left(\sqrt{2/3}\delta\phi_A + r\frac{2\pi}{3}\right), \qquad r = 0, \pm 1. \quad (12)$$

The DCK model reduces to three decoupled boundary sine-Gordon models [77–80], related to each other by a $\mathbb{Z}_3$ circular shift of the field $\delta\phi_A \to \delta\phi_A + 2\pi/\sqrt{6}$. They all have the same Bethe-ansatz solution describing the crossover from high to low energies (the same crossover as an impurity in a one-dimensional electron gas with Luttinger parameter $K = 1/3$ [77]). In particular, the residual entropy is predicted [81,82] to decrease by $\Delta S = \frac{1}{2}\ln(3)$ along the crossover. For the DCK model we therefore expect a crossover in the impurity entropy from $\ln(3)$ to $\frac{1}{2}\ln(3)$, as confirmed by the NRG results in Fig. 2(a). The parafermions σ and σ' generate the threefold charge subspace. Since σ' is screened but σ remains free, it simply halves the residual entropy. The same residual entropy was found in the quasiballistic limit [74].

Conductance at the critical point.—The linear conductance between left and right leads is obtained from the Kubo formula $G = -\lim_{\omega\to 0}[\mathrm{Im}K(\omega)/\omega]$, with $K(\omega)$ the Fourier transform of the retarded current-current correlator $K(t) = -i\theta(t)\langle[I(t), I(0)]\rangle$. Following the above mapping, $I = -(e/2\pi)\sqrt{\frac{2}{3}}\partial_t\Theta_A$, where Θ_A is the field conjugate to $\delta\phi_A$. Since $\delta\phi_A$ is pinned at the critical fixed point, Θ_A is free, and so $\langle\Theta_A(t)\Theta_A(0)\rangle \sim -\ln t$ at $T = 0$. This yields $G = G_0 = e^2/3h$: out of the three fields, only ϕ_A appears in Eq. (9), thus only Θ_A transports electrons, yielding $1/3$ of a perfect conductance.

Conductance scaling in the Kondo regime, $T \ll T_K$.—We now turn to the leading finite-temperature corrections to the $T = 0$ conductance at the critical point. To do this, we must perturb away from the exactly solvable EK point by reintroducing finite $\bar{\lambda}$. This is because the RG flow to the critical fixed point is affected by $\bar{\lambda}$. The leading irrelevant operator (LIO) at the QCP is given by $\mathcal{O}_{\mathrm{LIO}} = \bar{\lambda}[S_L^z \partial_x \delta\phi_1(0) + S_R^z \partial_x \delta\phi_2(0)]$. As we show in [61], the operators $\partial_x \delta\phi_{1,2}(0)$ both have scaling dimension 1 and $S_{L,R}^z$ have scaling dimension $\frac{1}{3}$. This yields $\Delta_{\mathrm{LIO}} = 4/3$, and therefore allows us to identify the leading correction to conductance (arising at order $\bar{\lambda}^2$) as $\delta G \sim (T/T_K)^{2(\Delta_{\mathrm{LIO}}-1)}$ [61], which reproduces Eq. (3a).

FL crossover.—The QCP is destabilized by gate voltage detuning away from the TP (appearing as pseudo-Zeeman fields $h_{L,R}$ in the DCK model), or by channel anisotropy δJ. The resulting FL crossover is controlled by the FL scale T^*. Assuming $T^* \ll T_K$, we may again utilize the Toulouse limit and set $\bar{\lambda} = 0$ to analyze the FL crossover, since any finite $\bar{\lambda}$ scales to zero anyway under RG for $T \ll T_K$. Both perturbations $h_{L,R}$ and δJ have the effect of coupling the otherwise independent sectors of H_{EK} given by Eq. (12). We focus here on finite h_R for simplicity. From Eq. (1), h_R couples to S_R^z, which in the rotated basis is given by

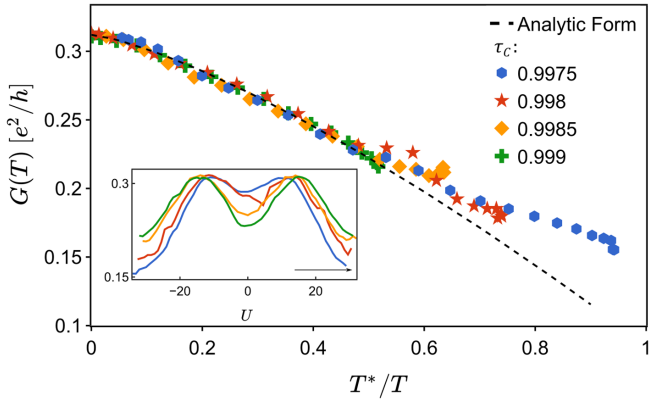

FIG. 3. Scaling collapse of experimental data from Ref. [60] (points) onto the asymptotic form of Eq. (13) (dashed line). Experiment performed for $\tau = 0.95$ at $T = 20$ mK with different τ_C . Inset shows experimental data along a line cutting through the pair of triple points. The main figure data are taken from a subset of this, starting at a triple point and moving toward higher U, indicated by the arrow. This avoids the discontinuity near $U = 0$ in the red curve, associated with a charge switching event. See [60,61] for experimental details, determination of T^*, and fitting procedure.

$S_R^z = \frac{1}{3}(\omega\tau + \omega^*\tau^\dagger)$. Analyzing its action at the QCP [61], we identify $\tau = e^{-i\sqrt{2/3}\Theta_A}$, where this operator circularly permutes the sectors r in Eq. (12). S_R^z thus inherits the RG-relevant scaling dimension $\Delta_R = 1/3$ of τ, such that finite h_R generates a FL scale $T^* \sim h_R^{1/(1-\Delta_R)}$. Since S_L^z and δJ have the same scaling dimension Δ_R, in general we have $T^* \sim (h_L^{3/2}, h_R^{3/2}, \delta J^{3/2})$ [61], which reduces to Eq. (2) in the case of pure channel anisotropy. The leading correction in T/T^* to the QCP conductance G_0 then follows as $\delta G \sim (T/T^*)^{2(\Delta_R-1)}$, yielding Eq. (3b). Additionally, the free parafermion at the QCP is shown by noise calculation [61] to scatter fractional charges $e^* = e/3$.

Comparison with experiment.—Finally, we turn to the implications of our results for the experiments of Ref. [60]. Although the experimental results were obtained at large transmission τ, τ_C, we expect the universal low-temperature behavior near the QCP to be the same as that discussed above for the Kondo limit [61,74]. Since the maximum conductance measured is slightly lower than the predicted value $G_0 = e^2/3h$, we infer that the quantum critical state is not fully developed at experimental base temperatures. Detuning away from the TP by varying the island gate voltages U generates a pseudo-Zeeman field $h_L = h_R$ in the DCK model, whereas detuning QPC transmission τ_C (while keeping τ constant) maps to channel anisotropy δJ. Either destabilizes the QCP and generates a finite FL scale T^*. Without perfect scale separation, we expect

$$G_0 - G(T) \sim c_K(T/T_K)^{2/3} + c_*(T/T^*)^{-4/3}. \quad (13)$$

In Fig. 3 we plot the experimental data vs T^*/T, with T^* estimated [60,61] for each combination of τ_C and U, while $T = 20$ mK is kept fixed. The rescaled data compare well with Eq. (13), when $c_K/T_K^{2/3}$ and c_* are used as free fit parameters. This provides strong evidence that the vicinity of the QCP in the DCK model is probed experimentally in the device of Ref. [60].

Conclusion and outlook.—The two-site charge-Kondo setup described by the DCK model can in the Toulouse limit be mapped to a solvable boundary sine-Gordon model by bosonization methods. At the QCP we show that the residual entropy $\frac{1}{2}\ln(3)$ is due to a free $\mathbb{Z}_3$ parafermion, while a second parafermion mode is Kondo screened. Exploiting the mapping, we also obtain exact results for the conductance near the critical point that agree not only with NRG results but also with experimental data. This suggests that a $\mathbb{Z}_3$ parafermion is already present in the experimentally measured device of Ref. [60]. This could be demonstrated more explicitly by measuring experimentally the fractional entropy of the parafermion using the methods proposed and implemented in Refs. [83–85]. Our approach also opens the door to studying other phases of quantum matter with irreducible strong interactions using the Emery-Kivelson mapping.

This work was supported by the Irish Research Council through the Laureate Award 2017/2018 Grant No. IRCLA/2017/169 (A. K. M.) and the French National Research Agency (project SIMCIRCUIT, ANR-18-CE47-0014-01). Analysis and extraction of experimental data compared to scaling theory in Fig. 3 was supported by the U.S. Department of Energy (DOE), Office of Science, Basic Energy Sciences (BES), under Contract No. DE-AC02-76SF00515.

*Present address: Materials Science Division, Argonne National Laboratory, Argonne, Illinois 60439, USA.
†Andrew.Mitchell@UCD.ie
‡christophe.mora@u-paris.fr

[1] A. Hewson, *The Kondo Problem to Heavy Fermions* (Cambridge University Press, Cambridge, United Kingdom, 1993).
[2] J. Kondo, Prog. Theor. Phys. **32**, 37 (1964).
[3] T. A. Costi, L. Bergqvist, A. Weichselbaum, J. Von Delft, T. Micklitz, A. Rosch, P. Mavropoulos, P. H. Dederichs, F. Mallet, L. Saminadayar, and C. Bauerle, Phys. Rev. Lett. **102**, 056802 (2009).
[4] D. Goldhaber-Gordon, H. Shtrikman, D. Mahalu, D. Abusch-Magder, U. Meirav, and M. A. Kastner, Nature (London) **391**, 156 (1998).
[5] S. M. Cronenwett, T. H. Oosterkamp, and L. P. Kouwenhoven, Science **281**, 540 (1998).
[6] W. Van der Wiel, S. D. Franceschi, T. Fujisawa, J. Elzerman, S. Tarucha, and L. Kouwenhoven, Science **289**, 2105 (2000).
[7] W. Liang, M. P. Shores, M. Bockrath, J. R. Long, and H. Park, Nature (London) **417**, 725 (2002).

[8] L. H. Yu, Z. K. Keane, J. W. Ciszek, L. Cheng, J. M. Tour, T. Baruah, M. R. Pederson, and D. Natelson, Phys. Rev. Lett. **95**, 256803 (2005).
[9] A. Georges, G. Kotliar, W. Krauth, and M. J. Rozenberg, Rev. Mod. Phys. **68**, 13 (1996).
[10] P. Nozieres and A. Blandin, J.Phys. **41**, 193 (1980).
[11] D. L. Cox and A. Zawadowski, Adv. Phys. **47**, 599 (1998).
[12] M.-S. Choi, R. López, and R. Aguado, Phys. Rev. Lett. **95**, 067204 (2005).
[13] J. Paaske, A. Rosch, P. Wölfle, N. Mason, C. Marcus, and J. Nygård, Nat. Phys. **2**, 460 (2006).
[14] N. Roch, S. Florens, T. A. Costi, W. Wernsdorfer, and F. Balestro, Phys. Rev. Lett. **103**, 197202 (2009).
[15] B. Béri and N. R. Cooper, Phys. Rev. Lett. **109**, 156803 (2012).
[16] M. R. Galpin, A. K. Mitchell, J. Temaismithi, D. E. Logan, B. Béri, and N. R. Cooper, Phys. Rev. B **89**, 045143 (2014).
[17] A. Keller, S. Amasha, I. Weymann, C. Moca, I. Rau, J. Katine, H. Shtrikman, G. Zaránd, and D. Goldhaber-Gordon, Nat. Phys. **10**, 145 (2014).
[18] A. K. Mitchell, K. G. Pedersen, P. Hedegård, and J. Paaske, Nat. Commun. **8**, 1 (2017).
[19] A. K. Mitchell, A. Liberman, E. Sela, and I. Affleck, Phys. Rev. Lett. **126**, 147702 (2021).
[20] M. Vojta, Philos. Mag. **86**, 1807 (2006).
[21] B. A. Jones, C. M. Varma, and J. W. Wilkins, Phys. Rev. Lett. **61**, 125 (1988).
[22] I. Affleck and A. W. W. Ludwig, Phys. Rev. Lett. **68**, 1046 (1992).
[23] I. Affleck and A. W. W. Ludwig, Phys. Rev. B **48**, 7297 (1993).
[24] Y. Oreg and D. Goldhaber-Gordon, Phys. Rev. Lett. **90**, 136602 (2003).
[25] R. M. Potok, I. G. Rau, H. Shtrikman, Y. Oreg, and D. Goldhaber-Gordon, Nature (London) **446**, 167 (2007).
[26] A. K. Mitchell, T. F. Jarrold, and D. E. Logan, Phys. Rev. B **79**, 085124 (2009).
[27] A. J. Keller, L. Peeters, C. P. Moca, I. Weymann, D. Mahalu, V. Umansky, G. Zaránd, and D. Goldhaber-Gordon, Nature (London) **526**, 237 (2015).
[28] Z. Iftikhar, S. Jezouin, A. Anthore, U. Gennser, F. D. Parmentier, A. Cavanna, and F. Pierre, Nature (London) **526**, 233 (2015).
[29] Z. Iftikhar, A. Anthore, A. K. Mitchell, F. D. Parmentier, U. Gennser, A. Ouerghi, A. Cavanna, C. Mora, P. Simon, and F. Pierre, Science **360**, 1315 (2018).
[30] I. Affleck, Acta Phys. Pol. B **26**, 1869 (1995).
[31] N. Andrei and C. Destri, Phys. Rev. Lett. **52**, 364 (1984).
[32] V. J. Emery and S. Kivelson, Phys. Rev. B **46**, 10812 (1992).
[33] K. G. Wilson, Rev. Mod. Phys. **47**, 773 (1975).
[34] R. Bulla, T. A. Costi, and T. Pruschke, Rev. Mod. Phys. **80**, 395 (2008).
[35] J. Gan, Phys. Rev. Lett. **74**, 2583 (1995).
[36] E. Sela, A. K. Mitchell, and L. Fritz, Phys. Rev. Lett. **106**, 147202 (2011).
[37] A. K. Mitchell and E. Sela, Phys. Rev. B **85**, 235127 (2012).
[38] A. K. Mitchell, E. Sela, and D. E. Logan, Phys. Rev. Lett. **108**, 086405 (2012).
[39] A. Bayat, H. Johannesson, S. Bose, and P. Sodano, Nat. Commun. **5**, 3784 (2014).
[40] F. W. Jayatilaka, M. R. Galpin, and D. E. Logan, Phys. Rev. B **84**, 115111 (2011).
[41] K. A. Matveev, Zh. Eksp. Teor. Fiz. **99**, 1598 (1991) [K. A. Matveev, Sov. Phys. JETP **72**, 892 (1991)].
[42] K. A. Matveev, Phys. Rev. B **51**, 1743 (1995).
[43] V. Mourik, K. Zuo, S. M. Frolov, S. Plissard, E. P. Bakkers, and L. P. Kouwenhoven, Science **336**, 1003 (2012).
[44] S. Nadj-Perge, I. K. Drozdov, J. Li, H. Chen, S. Jeon, J. Seo, A. H. MacDonald, B. A. Bernevig, and A. Yazdani, Science **346**, 602 (2014).
[45] C. Nayak, S. H. Simon, A. Stern, M. Freedman, and S. Das Sarma, Rev. Mod. Phys. **80**, 1083 (2008).
[46] A. Hutter and D. Loss, Phys. Rev. B **93**, 125105 (2016).
[47] P. L. S. Lopes, I. Affleck, and E. Sela, Phys. Rev. B **101**, 085141 (2020).
[48] Y. Komijani, Phys. Rev. B **101**, 235131 (2020).
[49] D. Gabay, C. Han, P. L. S. Lopes, I. Affleck, and E. Sela, Phys. Rev. B **105**, 035151 (2022).
[50] M. Lotem, E. Sela, and M. Goldstein, Phys. Rev. Lett. **129**, 227703 (2022).
[51] R. Wakatsuki, M. Ezawa, Y. Tanaka, and N. Nagaosa, Phys. Rev. B **90**, 014505 (2014).
[52] A. M. Tsvelik and P. Coleman, Phys. Rev. B **106**, 125144 (2022).
[53] P. Coleman, A. Panigrahi, and A. Tsvelik, Phys. Rev. Lett. **129**, 177601 (2022).
[54] F. del Pozo, L. Herviou, and K. L. Hur, arXiv:2210.05024.
[55] J. Klinovaja and D. Loss, Phys. Rev. Lett. **112**, 246403 (2014).
[56] M. Cheng, M. Becker, B. Bauer, and R. M. Lutchyn, Phys. Rev. X **4**, 031051 (2014).
[57] L. Mazza, F. Iemini, M. Dalmonte, and C. Mora, Phys. Rev. B **98**, 201109(R) (2018).
[58] B. Béri, Phys. Rev. Lett. **119**, 027701 (2017).
[59] A. Altland, B. Béri, R. Egger, and A. Tsvelik, J. Phys. A **47**, 265001 (2014).
[60] W. Pouse, L. Peeters, C. L. Hsueh, U. Gennser, A. Cavanna, M. A. Kastner, A. K. Mitchell, and D. Goldhaber-Gordon, Nat. Phys. (2023).
[61] See Supplemental Material at http://link.aps.org/supplemental/10.1103/PhysRevLett.130.146201 for further details of: (i) the analytical results and their derivation; (ii) the numerical implementation with NRG; (iii) experimental details and data fitting; (iv) discussion of fractionalization in other Kondo models; (v) comparison between Kondo and quasiballistic limits. Refs. [76–85] are contained therein.
[62] M. Fabrizio and A. O. Gogolin, Phys. Rev. B **50**, 17732 (1994).
[63] A. Furusaki and K. A. Matveev, Phys. Rev. B **52**, 16676 (1995).
[64] T. Morel, June-Young M. Lee, H.-S. Sim, and C. Mora, Phys. Rev. B **105**, 075433 (2022).
[65] L. A. Landau, E. Cornfeld, and E. Sela, Phys. Rev. Lett. **120**, 186801 (2018).
[66] A. Weichselbaum and J. von Delft, Phys. Rev. Lett. **99**, 076402 (2007).
[67] A. K. Mitchell, L. A. Landau, L. Fritz, and E. Sela, Phys. Rev. Lett. **116**, 157202 (2016).
[68] M. R. Galpin, A. K. Mitchell, J. Temaismithi, D. E. Logan, B. Béri, and N. R. Cooper, Phys. Rev. B **89**, 045143 (2014).

[69] F. B. Anders and A. Schiller, Phys. Rev. B **74**, 245113 (2006).
[70] E. L. Minarelli, J. B. Rigo, and A. K. Mitchell, arXiv:2209.01208.
[71] I. Affleck, M. Oshikawa, and H. Saleur, Nucl. Phys. **B594**, 535 (2001).
[72] A. K. Mitchell, M. R. Galpin, S. Wilson-Fletcher, D. E. Logan, and R. Bulla, Phys. Rev. B **89**, 121105(R) (2014).
[73] K. M. Stadler, A. K. Mitchell, J. von Delft, and A. Weichselbaum, Phys. Rev. B **93**, 235101 (2016).
[74] D. B. Karki, E. Boulat, and C. Mora, Phys. Rev. B **105**, 245418 (2022).
[75] P. Fendley, J. Stat. Mech. (2012) P11020.
[76] J. Alicea and P. Fendley, Annu. Rev. Condens. Matter Phys. **7**, 119 (2016).
[77] C. L. Kane and M. P. A. Fisher, Phys. Rev. B **46**, 15233 (1992).
[78] C. de C. Chamon, D. E. Freed, and X. G. Wen, Phys. Rev. B **51**, 2363 (1995).
[79] P. Fendley, A. W. W. Ludwig, and H. Saleur, Phys. Rev. Lett. **74**, 3005 (1995).
[80] P. Fendley, A. W. W. Ludwig, and H. Saleur, Phys. Rev. B **52**, 8934 (1995).
[81] P. Fendley, H. Saleur, and N. P. Warner, Nucl. Phys. **B430**, 577 (1994).
[82] P. Fendley, M. Fisher, and C. Nayak, J. Stat. Phys. **126**, 1111 (2007).
[83] E. Sela, Y. Oreg, S. Plugge, N. Hartman, S. Lüscher, and J. Folk, Phys. Rev. Lett. **123**, 147702 (2019).
[84] T. Child, O. Sheekey, S. Lüscher, S. Fallahi, G. C. Gardner, M. Manfra, Y. Kleeorin, Y. Meir, and J. Folk, Phys. Rev. Lett. **129**, 227702 (2021).
[85] C. Han, Z. Iftikhar, Y. Kleeorin, A. Anthore, F. Pierre, Y. Meir, A. K. Mitchell, and E. Sela, Phys. Rev. Lett. **128**, 146803 (2022).